



CHORUS

This is the accepted manuscript made available via CHORUS. The article has been published as:

Fragile Magnetic Ground State in Half-Doped $\text{LaSr}_{\{2\}}\text{Mn}_{\{2\}}\text{O}_{\{7\}}$

J.-S. Lee, C.-C. Kao, C. S. Nelson, H. Jang, K.-T. Ko, S. B. Kim, Y. J. Choi, S.-W. Cheong, S. Smadici, P. Abbamonte, and J.-H. Park

Phys. Rev. Lett. **107**, 037206 — Published 15 July 2011

DOI: [10.1103/PhysRevLett.107.037206](https://doi.org/10.1103/PhysRevLett.107.037206)

Fragile Magnetic Ground State in Half-Doped $\text{LaSr}_2\text{Mn}_2\text{O}_7$

J.-S. Lee,^{1,*} C.-C. Kao,¹ C. S. Nelson,² H. Jang,³ K.-T. Ko,³ S. B. Kim,⁴ Y. J. Choi,⁵ S.-W. Cheong,^{4,5} S. Smadici,⁶ P. Abbamonte,⁶ and J.-H. Park^{3,7,†}

¹Stanford Synchrotron Radiation Lightsource, SLAC National Accelerator Laboratory, Menlo Park, CA 94025, USA

²National Synchrotron Light Source, Brookhaven National Laboratory, Upton, NY 11973, USA

³c_CCMR & Department of Physics, Pohang University of Science and Technology, Pohang 790-784, S. Korea

⁴PEM & Department of Physics, Pohang University of Science and Technology, Pohang 790-784, S. Korea

⁵R-CEM & Department of Physics and Astronomy, Rutgers University, Piscataway, NJ 08854, USA

⁶Physics Department & Frederick Seitz Materials Research Laboratory, University of Illinois, Urbana, IL 61801, USA

⁷Division of Advanced Materials Science, Pohang University of Science and Technology, Pohang 790-784, S. Korea

We investigated the orbital and antiferromagnetic ordering behaviors of the half-doped bilayer manganite $\text{La}_{2-2x}\text{Sr}_{1+2x}\text{Mn}_2\text{O}_7$ ($x \simeq 0.5$) using Mn $L_{2,3}$ -edge resonant soft x-ray scattering (RSXS). RSXS reveals the CE -type orbital order below $T_{oo} \simeq 220$ K, which shows partial melting behavior below $T_m \simeq 165$ K. We also found coexistence CE - and A -type antiferromagnetic (AFM) orders. Both orders involve the CE -type orbital order with nearly the same orbital character and are coupled with each other. These results manifest that the ground state with the CE -type AFM order is easily susceptible to destabilization into the A -type one even with a small fluctuation of the doping level, as suggested by the extremely narrow magnetic phase boundaries at $x \simeq 0.5 \pm 0.005$.

PACS numbers: 75.47.Lx, 75.25.Dk, 78.70.Ck

Bilayer manganite $\text{La}_{2-2x}\text{Sr}_{1+2x}\text{Mn}_2\text{O}_7$ has attracted much attention in the last two decades due to a variety of emerging phenomena such as colossal magnetoresistance, metal-insulator transition, magnetoelasticity, etc, involving intimate couplings of charge, orbital, spin, and lattice degrees of freedom [1–6]. These couplings result in a complex magnetic phase diagram of ferromagnetic (FM) as well as different antiferromagnetic (AFM) phases in variations of the doping level x and temperature [7–17]. For the half-doped case, the A -type AFM order was observed experimentally although the CE -type order is predicted in the Goodenough model [18] based on the orbital states originally proposed for doped manganites. Recently a careful doping control study, however, reported that the system has an exotic phase diagram very near the half doping with an extremely narrow AFM phase boundaries at $x \simeq 0.5 \pm 0.005$ — the CE -type within the boundaries but the A -type outside [19]. The study confirmed the predicted CE -type AFM order for the true half-doped $x = 0.5$ case, but such a narrow phase boundary, which indicates close competition of the two phases, is puzzling since the CE -type order is expected to be rather stable in the model, as also observed in other half-doped manganites.

$\text{La}_{2-2x}\text{Sr}_{1+2x}\text{Mn}_2\text{O}_7$ consists of MnO_2 magnetic bilayers between nonmagnetic (La,Sr)O layers [see Fig. 1(a)]. In the $x \approx 0.5$ case, Mn^{3+} and Mn^{4+} ions are ordered alternately in the MnO_2 bilayers, and the orbital of the additional e_g electron at the Mn^{3+} site becomes ordered in the checkerboard (zigzag) pattern, i.e., the orbital order (OO), below $T_{oo} \sim 210$ K. Based on the OO pattern, the magnetic spins can be ordered in either the CE - or A -type pattern [see Fig. 1(b)]. The

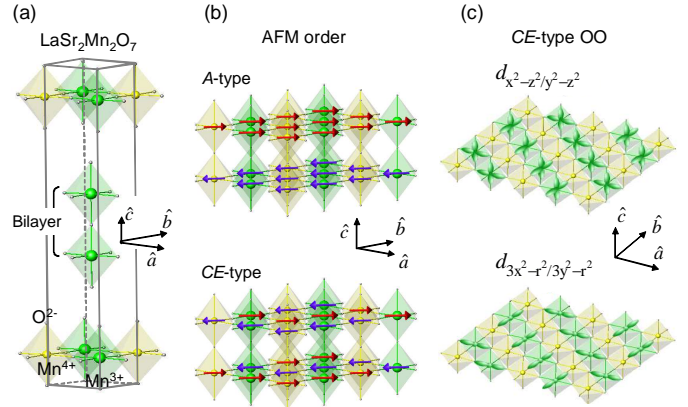


FIG. 1: (color online). (a) Crystal structure of bilayer $\text{LaSr}_2\text{Mn}_2\text{O}_7$. The gray lines denote a unit cell. (La,Sr)O layers are omitted for clarity. (b) A - (top) and CE -type (bottom) AFM spin structures. (c) two possibilities of CE -type OO (top: $d_{x^2-y^2}/y^2-z^2$ and bottom: $d_{3x^2-r^2}/3y^2-r^2$).

magnetic exchange interactions strongly depend on the orbital states, and the CE -type AFM order is expected to be favored in the $d_{3x^2-r^2}/3y^2-r^2$ -type orbital order as discussed in the model [18], while the A -type one is expected to be favored in the $d_{x^2-y^2}/y^2-z^2$ -type orbital order, which possibly activates the in-plane FM double exchange [see Fig. 1(c)]. Therefore, to understand the exotic phase diagram near $x = 0.5$ certainly requires information not only on the detailed ordering behaviors of the competing CE - and A -type AFM orders but also on the related orbital characters.

In this letter, we report details of orbital and magnetic ordering behaviors of half-doped bilayer manganite

$\text{La}_{2-2x}\text{Sr}_{1+2x}\text{Mn}_2\text{O}_7$ ($x \simeq 0.5$), in which the competing CE - and A -type AFM orders coexist. We use resonant soft x-ray scattering (RSXS) technique at the Mn $L_{2,3}$ -edge, which provides both the ordering and the electronic information. We observed large resonant enhancements at the reflection peaks of the CE -type ($\frac{1}{4}\frac{1}{4}0$) orbital order (OO) as well as the CE -type ($\frac{1}{4}\frac{1}{4}1$) and A -type (001) AFM orders. The OO reflection was found to be a composite of one involving the CE -type AFM order and the other involving the A -type one. The temperature dependence studies clearly show coupling behaviors of the coexisting CE - and A -type AFM orders, meaning that both AFM phases are not simply segregated. Examining the energy profiles of the OO peak and the x-ray absorption spectroscopy (XAS) spectra, we found that the e_g state involving the CE -type AFM order has nearly the same orbital character as that involving the A -type one. The orbital character is identified as a 2 : 1 mixture of $d_{3x^2-r^2}/3y^2-r^2$ and $d_{x^2-z^2}/y^2-z^2$ orbitals. These results strongly suggest the fragile magnetic ground state of the half-doped $\text{LaSr}_2\text{Mn}_2\text{O}_7$, in which the close competition of the CE - and A -type AFM ground states yields the extremely narrow phase boundaries.

The high quality $\text{LaSr}_2\text{Mn}_2\text{O}_7$ single crystals in a bilayered tetragonal structure ($I4/mmm$ space group) with lattice parameters of $a = b = 3.87 \text{ \AA}$, and $c = 20.0 \text{ \AA}$ were grown by the floating-zone method. The magnetic susceptibility (M/H) in Fig. 2(a) is very similar to that of the stoichiometry $\text{LaSr}_2\text{Mn}_2\text{O}_7$ reported earlier [19], and no noticeable change was observed in M/H after annealing in an O_2 circumstance, confirming the stoichiometry. For the RSXS measurements of the CE -type OO and AFM order, the sample was cut along the [110] direction and annealed for the surface reconstruction. For the measurements of the A -type AFM order and the x-ray absorption, the sample was cleaved *in situ* in a vacuum of $\sim 5 \times 10^{-10}$ Torr to expose a clean [00 L] surface. The sample size ($\sim 200 \times 700 \mu\text{m}^2$) was reduced to minimize the inhomogeneity problem in the stoichiometry [20]. The measurements were performed at the beamline X1B in National Synchrotron Light Source (NSLS). The incident photon polarization is 97% π -channel, and the XAS intensity was monitored simultaneously in the total electron yield mode.

We first investigated the orbital order (OO) using RSXS at Mn L -edge ($2p \rightarrow 3d$). At $T = 30 \text{ K}$, RSXS exhibits a resonance peak at the Bragg forbidden $\vec{q}_{oo} = (\frac{1}{4}\frac{1}{4}0)$ reflection as shown in Fig. 2(b). The coherence length was estimated to be $\sim 350 \text{ \AA}$ from the peak width. To understand the ordering behavior, we monitored the integrated intensity as a function of temperature [Fig. 2(d)]. The $\vec{q}_{oo} = (\frac{1}{4}\frac{1}{4}0)$ peak persists below $T_{oo} = 220 \text{ K}$. One can notice that the T -dependence shows anomalous behavior and can be separated into two different behaviors; one with a typical monotonic behavior [Fig. 2(e)] and the other with a melting behavior with

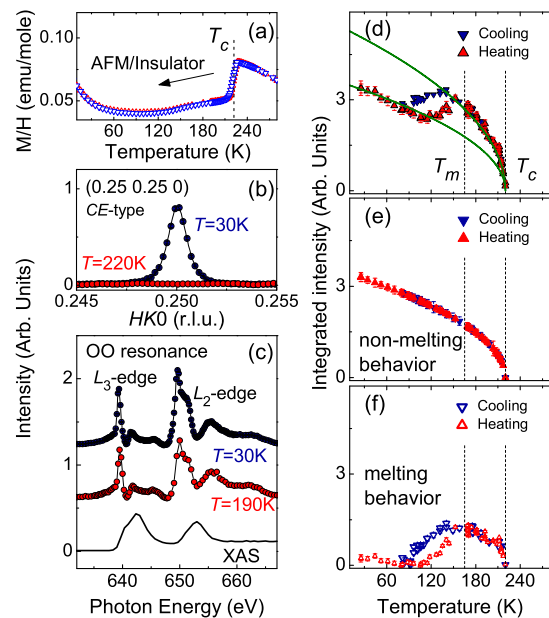


FIG. 2: (color online). (a) Magnetic susceptibility. (b) RSXS reflection for the CE -type OO at $T=30\text{K}$ and 220K ($h\nu = 638 \text{ eV}$) fitted with Gaussian and Lorentzian convoluted function (solid lines). (c) Energy profiles of RSXS for the CE -type OO above (190K) and below (30K) the melting behavior compared with the XAS spectrum. (d) Temperature dependence of the orbital order parameter. The green lines are the simple power law fits. (e) and (f) Separated two order parameters.

a thermal hysteresis for heating and cooling [Fig. 2(f)]. Here the T -dependence can be fitted to be a superposition of two power law $(1 - T/T_{oo})^\beta$ curves with a fixed $\beta \simeq 0.5$ and the 2 : 1 monotonic to hysteretic ratio (green solid curves in Fig. 2(d)). The melting behavior of OO was commonly observed in previous scattering studies on the near half-doped $\text{LaSr}_2\text{Mn}_2\text{O}_7$ with the A -type AFM order, in which it was attributed to development of the in-plane FM metallicity at T_m upon cooling [10–15]. The OO melting was found to be accompanied with the melting of the Mn^{3+} - Mn^{4+} charge order (CO) in the A -type AFM phase, resulting from the double exchange mechanism in the ab -plane, which reinforces the in-plane FM metallic phase [10, 19]. This result can be interpreted as the A -type AFM order developing with the OO melting behavior below $T_m \simeq 165 \text{ K}$ in a certain portion ($\sim 40\%$) of the sample, while OO involving the CE -type AFM order remains in the rest of the sample and persists to low temperature.

Now we explored the RSXS energy profile of the CE -type OO resonance, which provides the electronic information on the ordered state [21]. Figure 2(c) shows the energy profiles at 30 K and at 190 K together with the XAS spectrum as a reference. The XAS spectrum exhibits the typical Mn^{3+} - Mn^{4+} mixed valence features [22, 23], confirming the surface quality. In spite of the

fact that both orbital orders involving the *A*-type and *CE*-type AFM orders coexist at 190 K ($> T_m$) and the former OO melts down at 30 K, the energy profile exhibit nearly the identical line shape at both temperatures, taking into consideration the thermal effects. This result indicates that there is no significant difference in the e_g orbital character for both orders although they exhibits quite different T -dependent behaviors, in contrast to the previous expectation [see Fig. 1(c)] [18].

For direct investigation of the coexisting AFM orders, we performed the RSXS measurements at the reflections of the *A*-type AFM order $\vec{q}_{\text{AFM}}^A=(001)$ (Bragg forbidden) as well as the *CE*-type AFM order $\vec{q}_{\text{AFM}}^{CE}=(\frac{1}{4}\frac{1}{4}1)$ as shown in Fig. 3. We clearly observed the resonance peaks for both orders [Fig. 3(a)], and the coherence lengths were estimated to be ~ 900 Å [24]. Since the $\vec{q}_{\text{AFM}}^{CE}=(\frac{1}{4}\frac{1}{4}1)$ at the Mn L_3 -edge lies outside the Ewald sphere, the Mn L_2 -edge was utilized for the measurements. Nevertheless, one can recognize the difference in the energy profiles for the *CE*- and *A*-type AFM orders [Fig. 3(b)].

The temperature dependence of the integrated intensities for both AFM orders is presented in Fig. 3(c). The intensity for both orders mostly disappears at $T_N \simeq 165$

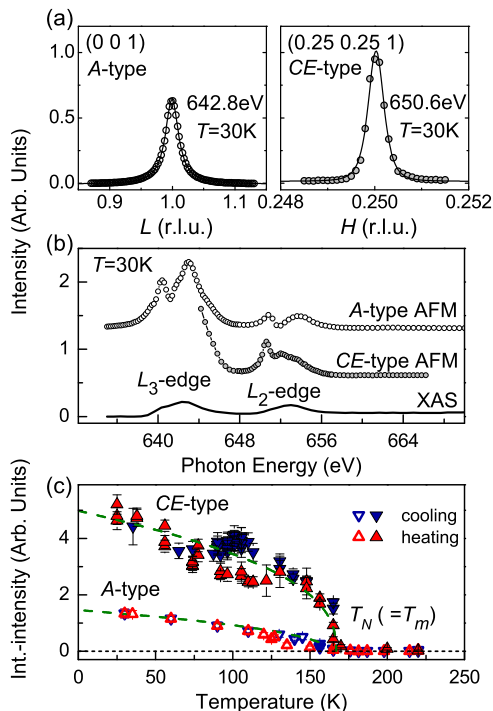


FIG. 3: (color online). AFM ordering behaviors of bilayer $\text{LaSr}_2\text{Mn}_2\text{O}_7$. (a) Forbidden reflections of the *A*-type and *CE*-type AFM orders at $T=30\text{K}$ fitted with Gaussian and Lorentzian convolution functions (solid lines). (b) RSXS energy profiles of the *A*-type and *CE*-type AFM order reflections compared with the XAS spectrum. (c) T -dependence of the *A*-type and *CE*-type AFM order parameters. The dashed lines are guide to the eye.

K, the same ordering temperature for the *CE*-type and *A*-type AFM order. It is noted that $T_N \simeq 165$ K is somewhat higher than $T_N \simeq 150$ K previously reported for the *CE*-type AFM order at $x = 0.5$, indicating that the x -value of our sample may be slightly away from the exact half-doping $x = 0.5$ or may have a slightly higher degree of regional fluctuation in the x -value although it is very similar in the magnetization behavior and in the OO temperature T_{oo} . $T_N \simeq 165$ K also coincides with T_m , at which the *CE*-type OO shows the melting behavior upon cooling [see Fig. 2(f)]. Furthermore, the *CE*-type AFM order parameter displays a thermal hysteresis in the temperature range, in which the *CE*-type OO parameter also shows the thermal hysteric behavior due to the OO melting [see Fig. 2(d) and (f)] involving the development of in-plane FM metallicity in the *A*-type AFM order. The thermal hysteresis is also observable in the *A*-type AFM order parameter although its signal is relatively small. These results show that the coexisting *CE*- and *A*-type AFM phases are not in simple phase segregation but coupled with each other. The coincidence in T_N of both phases indicates close energetics in their exchange couplings, and understanding of the coupling mechanism can be a perspective issue for the future study.

Although the energy profiles of the *CE*-type OO RSXS peak above and below T_m indicate that the orbital character is about the same for both *CE*-type and *A*-type AFM states [see Fig. 2(c)], more concrete information on the ordered e_g orbital is necessary to have an insight into the orbital and magnetic ordering behaviors. For this purpose, we performed the polarization dependent Mn $L_{2,3}$ XAS measurements at different temperatures as shown in Fig. 4(a). The XAS measurements were carried out at the elliptically polarized undulator beamline 2A at the Pohang Accelerator Laboratory (PAL). The total XAS intensity becomes somewhat larger for the incident photon polarization $\vec{E} \parallel \hat{c}$, implying more holes along the c -axis, and the size of the polarization dependence, the so-call linear dichroism (LD), gradually decreases as temperature increases. Even at low temperature, however, the LD size is much smaller than that expected for the in-plane $d_{3x^2-r^2}/3y^2-r^2$ orbital states [Fig. 1(c)] [25], indicating that the orbital character in the ground state is not purely the in-plane orbital states. For the quantitative characterization, we mimicked the polarization dependent XAS spectra, using the cluster model calculations with the full atomic multiplets [26]. As can be seen in Fig. 4(b), the calculated spectra well reproduce the measured ones including the gradual reduction of the LD size with temperature. From the calculation, the e_g orbital state in the ground state has a 2 : 1 mixture of $d_{3x^2-r^2}/3y^2-r^2$ and $d_{x^2-z^2}/y^2-z^2$ orbitals as presented in Fig. 4(c). The initial state mixing due to the thermal energy with the Boltzmann factor reproduces well the gradual reduction in the LD signal without any change in the ground state.

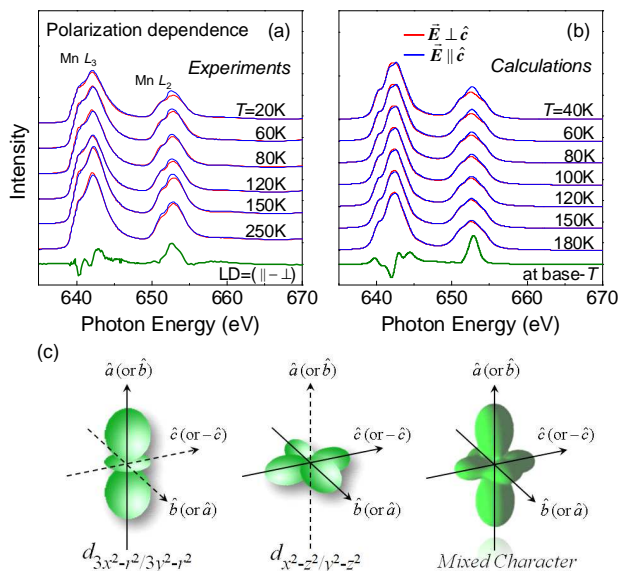


FIG. 4: (color online). (a) Polarization dependent XAS spectra and LD at base temperature, and (b) Cluster model calculations. (c) Schematic diagrams of orbital states for $\text{LaSr}_2\text{Mn}_2\text{O}_7$. The mixed character shows the 2 : 1 mixture of $d_{3x^2-r^2}/3y^2-r^2$ and $d_{x^2-z^2}/y^2-z^2$ orbitals.

In the MnO_6 octahedron, the Mn^{3+} Jahn-Teller (JT) distortion usually favors the $d_{3z^2-r^2}$ orbital state for the additional e_g electron, and the $d_{3x^2-r^2}/3y^2-r^2$ pattern forms the CE -type OO in the half-doped perovskite manganites (3D) [18, 27]. Meanwhile, in the single layer $\text{La}_{0.5}\text{Sr}_{1.5}\text{MnO}_4$ (2D), the $d_{3x^2-r^2}/3y^2-r^2$ pattern competes with the uniaxial structural distortion, and the system stabilizes the CE -type OO with the $d_{x^2-z^2}/y^2-z^2$ pattern [25, 28] even though this strengthens the double exchange mechanism. In fact, the zigzag chains under CE -OO/ A -AFM order couple ferromagnetically in-plane, while they couple antiferromagnetically in CE -OO/ CE -AFM order. It could hypothesize that the planes are in turn coupled antiferromagnetically reduce the A -type AFM structure. Thus, the mixed orbital character seems to be quite natural in the bilayer $\text{LaSr}_2\text{Mn}_2\text{O}_7$ possessing both the 2D and 3D like characteristics. In the aspect of the magnetic interaction, the anisotropic orbital state stabilizes the CE -type AFM order ($d_{3x^2-r^2}/3y^2-r^2$ in the 3D and $d_{x^2-z^2}/y^2-z^2$ in the 2D), while the isotropic orbital state with the 1:1 mixture maximizes the Mn^{3+} - Mn^{4+} double exchange mechanism to stabilize the FM metallic states. Hence in the 2 : 1 mixed orbital character, the CE -type AFM ground state is energetically very close to the A -type AFM state at $x = 0.5$, resulting in the fragile CE -type AFM ground state with the extremely narrow phase boundaries. Consequently, even a tiny deviation in the x -value induces the OO melting and stabilizes the A -type AFM order balancing the in-layer FM metallicity and the inter-layer AFM

order among the MnO_2 bilayer. Such an orbital instability offers a rich opportunity for detailed experimental and theoretical investigations.

In summary, we report detailed studies of the orbital and magnetic ordering behaviors of $\text{La}_{2-2x}\text{Sr}_{1+2x}\text{Mn}_2\text{O}_7$ ($x \simeq 0.5$). The ground state for $x = 0.5$ is the CE -type AFM state in a close competition with the A -type one. The e_g orbital state stays as a 2 : 1 mixture of $d_{3x^2-r^2}/3y^2-r^2$ and $d_{x^2-z^2}/y^2-z^2$ without significant change for both magnetic states. This mixed orbital state leads to the fragile magnetic ground state, and a tiny deviation in the doping level causes a change of the AFM type ($CE \rightarrow A$).

We thank Stuart Wilkins for useful discussions. RSXS studies were supported by Office of Basic Energy Sciences, U.S. DOE under Grant No. DE-FG02-06ER46285, with use of the NSLS supported under Contract No. DE-AC02-98CH10886. The work at POSTECH is supported by the NCIC for c-CCMR (2009-0081576), WCU program (R31-2008-000-10059-0), and LFRIR program (2010-00471) through NRF funded by MEST. l -PEM is supported by POSTECH, and PAL is supported by POSTECH and MOST.

* Electronic address: jslee@slac.stanford.edu

† Electronic address: jhp@postech.ac.kr

- [1] S. Jin, *Science* **264**, 413 (1994).
- [2] Y. Moritomo *et al.*, *Nature* **380**, 141 (1996).
- [3] S.-W. Cheong *et al.*, *Nature Mater.* **6**, 13 (2007).
- [4] M. Coey, *Nature* **430**, 155 (2004).
- [5] J. M. D. Coey *et al.*, *Adv. in Phys.* **48**, 167 (1999).
- [6] E. Dagotto, *Science* **309**, 257 (2005).
- [7] K. Ueda *et al.*, *Science* **280**, 1064 (1998).
- [8] J. Chakhalian, *Science* **318**, 1114 (2007).
- [9] S.-W. Cheong, *Nature Mater.* **6**, 927 (2005).
- [10] T. Kimura *et al.*, *Phys. Rev. B* **58**, 11081 (1998).
- [11] D. N. Argyriou *et al.*, *Phys. Rev. B* **61**, 15269 (2000).
- [12] T. Chatterji *et al.*, *Phys. Rev. B* **61**, 570 (2000).
- [13] M. Kubota *et al.*, *J. Phys. Soc. Jpn.* **68**, 2202 (1999).
- [14] C. D. Ling *et al.*, *Phys. Rev. B* **62**, 15096 (2000).
- [15] Y. Wakabayashi *et al.*, *J. Phys. Soc. Jpn.* **72**, 618 (2003).
- [16] S. B. Wilkins *et al.*, *Phys. Rev. B* **67**, 205110 (2003).
- [17] F. Weber *et al.*, *Nature Mater.* **8**, 798 (2009).
- [18] J. B. Goodenough, *Phys. Rev.* **100**, 564 (1955).
- [19] Q. Li *et al.*, *Phys. Rev. Lett.*, **98**, 167201 (2007).
- [20] H. Zheng *et al.*, *Phys. Rev. B* **78**, 155103 (2008).
- [21] S. Ishihara *et al.*, *Phys. Rev. Lett.* **80**, 3799 (1998); S. B. Wilkins *et al.*, *Phys. Rev. B* **71**, 245102 (2005).
- [22] M. Abbate *et al.*, *Phys. Rev. Lett.* **46**, 4511 (1992).
- [23] C. Aruta *et al.*, *Eur. Phys. Lett.* **80**, 37003 (2007).
- [24] The orbital and spin orders have different coherence lengths as other manganites [J.P. Hill *et al.*, *Appl. Phys. A* **73**, 723 (2001)].
- [25] D. J. Huang *et al.*, *Phys. Rev. Lett.* **92**, 087202 (2004).
- [26] A. Tanaka and T. Jo, *J. Phys. Soc. Jpn.* **63**, 2788 (1994).
- [27] P. G. Radaelli *et al.*, *Phys. Rev. Lett.* **75**, 4488 (1995).
- [28] S. B. Wilkins *et al.*, *Phys. Rev. Lett.* **91**, 167205 (2003).